

From polyester grafting onto POSS nanocage by ring-opening polymerization to high performance polyester/POSS nanocomposites†

Anne-Lise Goffin,^a Emmanuel Duquesne,^a Jean-Marie Raquez,^{*a} Hans E. Miltner,^b Xiaoxing Ke,^c Michaël Alexandre,^{‡a} Gustaaf Van Tendeloo,^c Bruno Van Mele^b and Philippe Dubois^{*a}

Received 3rd February 2010, Accepted 14th April 2010

DOI: 10.1039/c0jm00283f

Polyester-grafted polyhedral oligomeric silsesquioxane (POSS) nanohybrids selectively produced by ring-opening polymerization of ϵ -caprolactone and L,L-lactide (A.-L. Goffin, E. Duquesne, S. Moins, M. Alexandre, Ph. Dubois, *Eur. Polym. Journal*, 2007, **43**, 4103) were studied as “masterbatches” by melt-blending within their corresponding commercial polymeric matrices, *i.e.*, poly(ϵ -caprolactone) (PCL) and poly(L,L-lactide) (PLA). For the sake of comparison, neat POSS nanoparticles were also dispersed in PCL and PLA. The objective was to prepare aliphatic polyester-based nanocomposites with enhanced crystallization behavior, and therefore, enhanced thermo-mechanical properties. Wide-angle X-ray scattering and transmission electron microscopy attested for the dispersion of individualized POSS nanoparticles in the resulting nanocomposite materials only when the polyester-grafted POSS nanohybrid was used as a masterbatch. The large impact of such finely dispersed (grafted) nanoparticles on the crystallization behavior for the corresponding polyester matrices was noticed, as evidenced by differential scanning calorimetry analysis. Indeed, well-dispersed POSS nanoparticles acted as efficient nucleating sites, significantly increasing the crystallinity degree of both PCL and PLA matrices. As a result, a positive impact on thermo-mechanical properties was highlighted by *dynamic mechanical thermal analysis*.

Introduction

The introduction of nano-sized inorganic reinforcements has appeared to be an efficient way to modify and to improve the properties of polymer-based materials. These so-called polymeric nanocomposites exhibit enhanced polymer performances such as stiffness even at very low nanofiller contents (a few wt%). Throughout the past decade, polyhedral oligomeric silsesquioxanes (POSS) have been increasingly studied as a reinforcing isotropic nanofiller (*i.e.*, with dimensions in the range of 1 to 3 nm)^{2,3} for their ability to improve the thermal, crystalline,⁴⁻⁷ mechanical,^{8,9} barrier^{10,11} and fire-resistance¹²⁻¹⁴ properties of polymeric materials. Typically, a POSS nanoparticle can be represented as a cage-like siloxane structure surrounded by eight organic R groups. POSS nanoparticles can bear different types of substituents (R reactive or non-reactive). When the R groups are non-reactive such as alkyl groups, this allows for a good

nanofiller “solubilization” into the polymer matrix, but rather limited to polyolefins.¹⁵ Due to the predominant POSS-POSS interactions towards POSS-polymer interactions,¹⁶ POSS nanoparticles tend to aggregate when they are melt-blended within polymer matrices. Such aggregated microstructure could lead to brittle materials. In order to limit aggregation, using POSS nanoparticles with reactive (or even polymerizable) R substituents represents an interesting way to improve the compatibility of POSS with polymeric materials through nanoparticles surface modification. This gives access to new inorganic-organic nanohybrids with improved properties. Some of the POSS surface chemical modifications include functionalization,^{17,18} cross-linking,¹⁶⁻²¹ polymer grafting²²⁻³⁰ or reactive blending.³¹ Of all these reactive pathways, the formation of a covalent bond between the filler and the polymer matrix by “grafting from” polymerization should be pointed out.^{32,33} In this method, the polymer chains are synthesized by *in situ* polymerization surface-initiated from functionalized nanoparticles. High grafting densities can be achieved without limitation in grafted-polymer molar mass in contrast to, *e.g.*, “grafting onto” methods. When dispersed in a polymeric matrix miscible or compatible with the surface-grafted polymer chains, chain entanglements take place at the nanoparticle/matrix interphase, which can even trigger (co)crystallization with polymer chains of the host matrix leading to excellent interface adhesion. Accordingly, numerous matrices such as polyolefins, polysiloxanes, poly(meth)acrylates and polyesters have been grafted onto POSS following different polymerization mechanisms like ring-opening polymerization,^{1,26,28,30} ring-opening metathesis polymerization²⁵ and atom transfer radical polymerization.^{27,34,35} Our group has recently reported the synthesis of well-defined POSS-based nanohybrids

^aLaboratory of Polymeric and Composite Materials (LPCM), Center of Innovation and Research in Materials and Polymers (CIRMAP), University of Mons - UMONS, Place de Parc 20, 7000 Mons, Belgium. E-mail: Jean-Marie.Raquez@umons.ac.be; Philippe.Dubois@umons.ac.be; Fax: +3265373484; Tel: +3265373480

^bPhysical Chemistry and Polymer Science, Vrije Universiteit Brussel, Pleinlaan 2, B-1050 Brussels, Belgium

^cElectron Microscopy for Materials Science, Universiteit Antwerpen, Groenenborgerlaan 171, B-2020 Antwerpen, Belgium

† This paper is part of a *Journal of Materials Chemistry* themed issue on Advanced Hybrid Materials, inspired by the symposium on Advanced Hybrid Materials: Stakes and Concepts, E-MRS 2010 meeting in Strasbourg. Guest editors: Pierre Rabu and Andreas Taubert.

‡ Current address: Center for Education and Research on Macromolecules, University of Liège, B6a Sart Tilman, 4000 Liège, Belgium

as obtained by ring-opening polymerization of ϵ -caprolactone (CL) and L,L-lactide (L,L-LA) initiated by amino-functionalized POSS using tin(II) octoate ($\text{Sn}(\text{oct})_2$) as a catalyst.¹ Selective initiation and control over the molecular parameters of the grafted polyester chains have been demonstrated.

Recently, it was demonstrated that POSS-based nanohybrids as synthesized by the “grafting from” approach, *e.g.*, poly(ϵ -caprolactone) (PCL)-grafted POSS (POSS-*g*-PCL), could significantly modify the crystallization process of the grafted polymer chains,^{28,36,37} even without dilution in a commercial matrix. This nucleating effect provided by POSS nanoparticles on the covalently grafted chains is interesting in order to tune up the crystalline properties of the materials. However, a high number (max. 8) of grafted chains per POSS nanocage and/or very long polymer grafts are required, producing nanohybrids with low POSS content (*e.g.*, below 5 wt%) and relevant thermomechanical properties. Interestingly enough, dilution of the so-produced POSS-*g*-polyester nanohybrids within well-selected polymer matrices should represent a good alternative. Nevertheless, only few reports have dealt with the formation and properties of such nanohybrid-based nanocomposite materials. For instance, Qian and Zheng's group reported the preparation of epoxy-based nanocomposites filled with POSS-*g*-PCL, yielding nanostructured organic-inorganic hybrids.³⁸

Hence, this contribution aims to study the reinforcing effect, especially the nucleating effect, provided by polyester-grafted POSS nanohybrids (*vide supra*)¹ on the thermal and thermo-mechanical properties of the corresponding commercial matrices, *i.e.*, poly(ϵ -caprolactone) (PCL) and poly(L,L-lactide) (PLA) in order to prepare high-performance polyester/POSS nanocomposites. Different polyester-grafted POSS contents were investigated by melt-blending these polyester-grafted nanohybrids thus obtained by ROP of L,L-LA or CL, as masterbatches, within their corresponding commercial polymers using a twin-screw microcompounder. In addition to their biodegradability, PCL and PLA have been chosen due to their particular crystalline properties. Actually, a PCL matrix is a well-crystallizable polymer ($T_g \approx -60^\circ\text{C}$ and $T_m \approx 60^\circ\text{C}$), as opposed to PLA ($T_g \approx 55^\circ\text{C}$ and $T_m < 170^\circ\text{C}$ depending on the residual D,D-lactide content). Indeed, PLA-based materials are known to be difficult to efficiently crystallize during their melt-processing at the industrial level. Due to its inherent biodegradability and renewability, such a behavior restricts the huge potentiality of PLA, especially where the end-life of this polymer concerns short-time applications. In this respect, we purposely studied a PLA commercial sample that contains a D,D-LA content as high as 10 wt% drastically limiting its crystallization properties. The first part of this study was devoted to the nucleating effect of POSS-based nanoparticles on the thermal and thermo-mechanical properties of commercial PCL. The “model study” concerning PCL was then extended to the PLA matrix in order to provide clear-cut evidence for the nucleating effect of the corresponding POSS-*g*-PLA nanohybrids. To highlight on one hand the reinforcement provided by the quality of the POSS dispersion, and on the other hand their effect on both thermal and thermo-mechanical properties of the polyester matrices, differential scanning calorimetry (DSC), wide angle X-ray scattering (WAXS), transmission electron microscopy (TEM) and dynamic mechanical thermal analysis (DMTA) were used as

characterization tools. Effect of polyester-grafted POSS on the materials properties was further compared with compositions based on neat (non-grafted) POSS blended within the same polyester matrices.

Experimental section

Materials

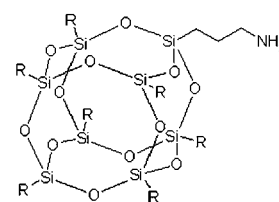
Aminopropylheptakis(isobutyl)POSS (amino-POSS or aPOSS, Fig. 1) and octaisobutyl-POSS (ⁱBut-POSS or iPOSS, Fig. 2) were purchased from Hybrid Plastics and used as received. Commercial grade PCL (CAPA6500, $M_n = 50,000 \text{ g mol}^{-1}$) and PLA (4032D) were supplied by Solvay and NatureWorks, respectively. PLA 4032D was characterized by an average molecular weight of $52,000 \text{ g mol}^{-1}$, a polydispersity (M_w/M_n) of 1.9, and an L/D isomer ratio of 90/10. DSC analysis (*vide infra*) of this neat PLA sample showed the absence of any crystallization/melting peak, attesting for its amorphous character (at least under our experimental conditions).

Preparation of polyester-based (nano)composites

All details concerning the synthesis of polyester-grafted aPOSS nanohybrids have been recently reported.¹ Table 1 reports ROP conditions and nanohybrids compositions for the PCL and PLA based materials.

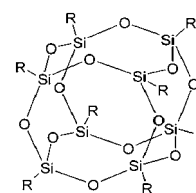
CAPA6500/POSS (nano)composites were prepared by melt-blending in a ThermoHaake MiniLab Rheomex CTW5 mini-extruder at 90°C and 75 rpm for 10 min. Then, rectangular samples ($35 \text{ mm} \times 12 \text{ mm} \times 3 \text{ mm}$) were prepared by injection-molding at 120°C for dynamical mechanical thermal analysis (DMTA).

For PLA4032D/POSS (nano)composite materials, the matrix was first dried under vacuum at 70°C for 4 h. Extrusion conditions were: 10 min at 180°C with a rotation speed of 150 rpm. Finally, DMTA samples were injection-molded at 200°C .



R = isobutyl

Fig. 1 An amino-POSS nanoparticle (aPOSS).



R = isobutyl

Fig. 2 An ⁱBu-POSS nanoparticle (iPOSS).

Table 1 ROP conditions and molecular parameters of the aPOSS-g-PCL and aPOSS-g-PLA nanohybrids as synthesized by ROP of CL ($[\text{CL}]_0/[\text{NH}_2]_0 = 80$; $[\text{NH}_2]_0/[\text{Sn}(\text{oct})_2]_0 = 2.5$; $[\text{CL}]_0 = 2\text{M}$; $T = 95^\circ\text{C}$; Time = 7 h) and L,L-LA ($[\text{LA}]_0/[\text{NH}_2]_0 = 80$; $[\text{NH}_2]_0/[\text{Sn}(\text{oct})_2]_0 = 2.5$; $[\text{LA}]_0 = 1\text{M}$; $T = 80^\circ\text{C}$; Time = 7 h), respectively

Monomer	DP _{RMN} ^a	M _n RMN ^a /g mol ⁻¹	aPOSS content (%)
CL	70	8000	10
LA	73	5200	14

^a as measured by ¹H NMR in CDCl₃.

Prior to DMTA measurement, all PLA samples (neat PLA and PLA-based (nano)composites) were annealed for 90 min at 110 °C.

Different materials were prepared (see Table 2): the unfilled matrices and corresponding (nano)composites: direct POSS dispersion (CAPA6500/aPOSS and PLA4032D/iPOSS) and polyester-grafted aPOSS dispersion as masterbatch (CAPA6500/aPOSS-g-PCL and PLA4032D/aPOSS-g-PLA) at inorganic contents of 3 and 5 wt%. An additional ternary composition was prepared, *i.e.*, by melt-blending CAPA6500, 5% aPOSS and an oligo-PCL with a degree of polymerization (DP ≈ 80) in the same range than the PCL chains grafted onto POSS nano-cages and added in the same relative content than in the aPOSS-g-PCL masterbatch (see results and discussion).

Characterization techniques

The morphology of the (nano)composites was analyzed by wide-angle X-ray scattering (WAXD) and transmission electron microscopy (TEM). WAXD patterns were recorded between 1.65° and 30° (by steps of 0.04°) with a Siemens D5000 diffractometer, operating with Cu-K α radiation ($\alpha = 1.5406\text{ \AA}$). For recording TEM images, the samples were cryomicrotomed at -100 °C by an Ultracut FC4E microtome from Reichert-Jung. High-resolution transmission electron microscopy (HRTEM) was carried out using a Philips CM20 microscope operated at 200 kV.

Dynamic mechanical thermal analyses (DMTA) of the nanocomposites were performed under ambient atmosphere using a 2980 DMTA apparatus from TA Instruments in a dual cantilever. The measurements were carried out at a constant frequency of 1 Hz, a temperature range from -100 to 30 °C for PCL-based materials and 0 to 140 °C for PLA at a heating rate of 3 °C min⁻¹. Three samples were characterized for each composition.

Table 2 Summary of polyester/POSS based materials prepared by melt-blending

Polyester matrix	Composition
CAPA6500	0%
CAPA6500	+ 3 and 5% aPOSS
CAPA6500	+ 3 and 5% aPOSS-g-PCL
CAPA6500	+ 5% oligo-PCL/aPOSS
PLA4032D	0%
PLA4032D	+ 5% iPOSS
PLA4032D	+ 5% aPOSS-g-PLA

Thermal characterizations using conventional and modulated temperature differential scanning calorimetry (MTDSC) were performed using a TA Instruments Q100 and Q2000 DSC, respectively. Concerning MTDSC analyses, the instrument was equipped with a refrigerated cooling system (RCS) for quasi-isothermal experiments, whereas a liquid nitrogen cooling system (LNCS) was used for non-isothermal experiments. The instrument was purged with helium (25 ml min⁻¹) or nitrogen gas (25 ml min⁻¹), respectively. Temperature and enthalpy calibration were performed using an indium standard; heat capacity calibration was performed using sapphire disks. The selected temperature modulation conditions were: amplitude of $\pm 0.5^\circ\text{C}$ and a period of 60 s. The glass transition temperature (T_g), crystallization temperature (T_c), enthalpy of crystallization or cold crystallization (for PLA) (ΔH_c) and melting enthalpy (ΔH_m) were determined from the second scan. The enthalpy values were calculated taking in account the proportion of inorganic compounds.

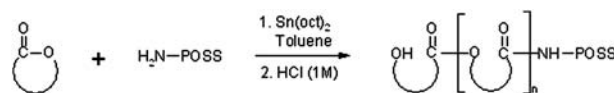
Results and discussion

Poly(ϵ -caprolactone)/POSS nanocomposites

A well-defined aPOSS-g-poly(ϵ -caprolactone) (aPOSS-g-PCL) nanohybrid was synthesized by ring-opening polymerization (ROP) of ϵ -caprolactone (CL) catalyzed by tin(II) 2-ethylhexanoate (tin octoate, Sn(oct)₂) at 95 °C.¹ The synthesis was selectively initiated from the primary amine groups³⁹ present on aminopropylheptakis(isobutyl)POSS nanoparticles (Scheme 1). In the present study, the resulting aPOSS-g-PCL has a degree of polymerization (DP) of 70 with an inorganic content around 10 mol%.

CAPA6500/aPOSS nanocomposites were then prepared by melt-blending using a twin-screw microcompounder at 3 and 5 wt% organic content of polyester-grafted aPOSS nanoparticles. For the sake of comparison, both aPOSS and a mixture of aPOSS and non-grafted oligo-PCL (with a DP in the range of 80) were directly melt-blended within the commercial PCL matrix (CAPA6500). The morphological properties were first studied by means of WAXS and TEM measurements. WAXS spectra (Fig. 3) present the characteristic peaks of PCL crystals at around $2\theta = 21.2^\circ$ and 23.5° .⁴⁰ As far as the CAPA6500/3%aPOSS (nano)composites are concerned, the presence of a diffraction peak at $2\theta = 8^\circ$ assigned to aPOSS self-associations, clearly indicates that aPOSS nanoparticles remain aggregated. Interestingly, this diffraction peak is not present for CAPA6500/3%aPOSS-g-PCL compositions, attesting for the complete individualization of grafted aPOSS nanoparticles within the commercial PCL matrix.

These observations were confirmed by high-resolution TEM analysis. Fig. 4a shows TEM images of non-grafted aPOSS nanoparticles, where aPOSS appears as cubic aggregates up to



Scheme 1 Ring-opening polymerization of cyclic esters as initiated by amino-POSS nanoparticles.

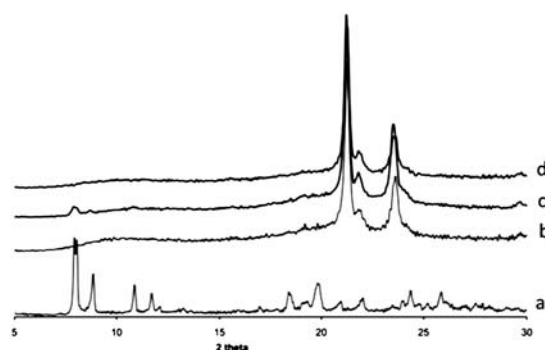


Fig. 3 WAXS spectra (presented upwards) of (a) aPOSS nanoparticles, (b) unfilled CAPA6500, (c) CAPA6500/3%aPOSS and (d) CAPA6500/3%aPOSS-g-PCLCL.

1 micron size. As observed by WAXS, (nano)composites filled with ungrafted aPOSS (Fig. 4b) reveal the presence of lower size aPOSS aggregates (~ 100 nm). Interestingly, grafting PCL onto amino-POSS nanoparticles leads to the total disaggregation of aPOSS nanoparticles. The resulting nanocomposites present homogeneous nanostructure (Fig. 4c). aPOSS nanoparticles ($d \approx 2$ nm) are undetectable because their size is close to the HR-TEM limits.

To show the extent of aPOSS dispersion on the (nano)-composite mechanical properties, DMTA analyses were performed on the unfilled PCL matrix and (aPOSS or aPOSS-g-PCL) filled (nano)composites. Fig. 5 shows the curves of isochronal evolution of the storage modulus (E') as a function of temperature. The unmodified PCL matrix shows the typical behavior of a semi-crystalline polymer with a glass transition at around -60 °C. Before T_g , the modulus slightly decreased, and remained roughly constant. At higher temperature, a rapid decrease of E' is noted around -50 °C, corresponding to the glass-rubber transition. This decrease in storage modulus is significantly attenuated, when aPOSS-g-PCL masterbatches are used. This observation is clearly illustrated by the modulus value at room temperature; E' increases by *ca.* 25% (Fig. 6) with respect to neat semi-crystalline PCL matrix. As well-shown by the morphological analyses, these results suggest that the covalent bond between the aPOSS nanocage and the PCL chain allows finely dispersing, and compatibilizing the POSS nanofillers with the commercial PCL matrix (CAPA6500). Such an observation may find some further supports from the thermal behavior, *i.e.*,

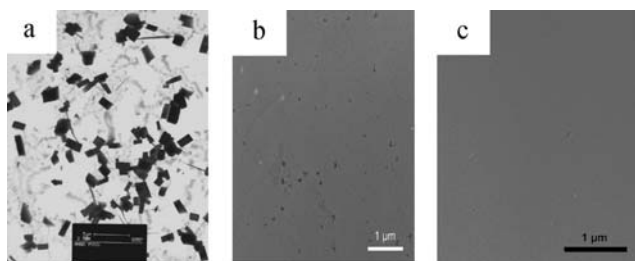


Fig. 4 TEM analysis of (a) aPOSS nanoparticles, (b) CAPA6500/3%aPOSS and (c) CAPA6500/3%aPOSS-g-PCL-based (nano)-composites.

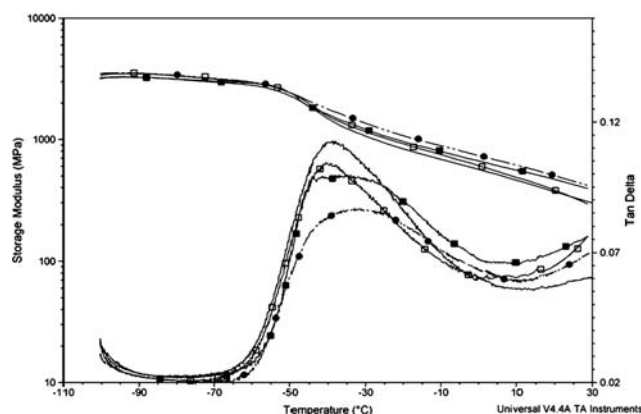


Fig. 5 Isochronal evolution of the storage modulus (E') vs. temperature of (–) unfilled CAPA6500, (□) CAPA6500/3%aPOSS and CAPA6500/3% and (●) 5% aPOSS-g-PCL.

the extent of crystallization as checked by differential scanning calorimetry (DSC).

Fig. 7 shows the DSC thermograms of PCL (nano)composites, compared with neat PCL. In the case of neat PCL, a melting temperature at 59 °C is observed with a crystallization peak at 32 °C. While getting melting temperatures comparable, addition of non-grafted aPOSS slightly increases the values of enthalpies of melting and crystallization. Interestingly, this increase is more marked for masterbatch-based materials, *i.e.*, nanocomposites obtained from aPOSS-g-PCL, reaching an enhancement of *ca.* 50% for CAPA6500/5%aPOSS-g-PCL. In order to highlight the effect of oligoPCL on the crystallization properties of commercial PCL, a ternary (CAPA6500/oligo-PCL/5%aPOSS) system was prepared, containing the same amount of oligo-PCL ($DP \sim 80$) as one in the aPOSS-g-PCL masterbatch. The crystallization and melting characteristics of the PCL matrix proved to be less increased than those recorded in the presence of the aPOSS-g-PCL masterbatch (Table 3). By comparison with the CAPA6500/5%aPOSS sample, it appears that the presence of non-grafted oligo-PCL fraction does not play any significant role on the thermal behavior of the polyester matrix. Only the covalent grafting of PCL onto aPOSS nanoparticles allows substantially enhancing the crystallinity of the PCL matrix.

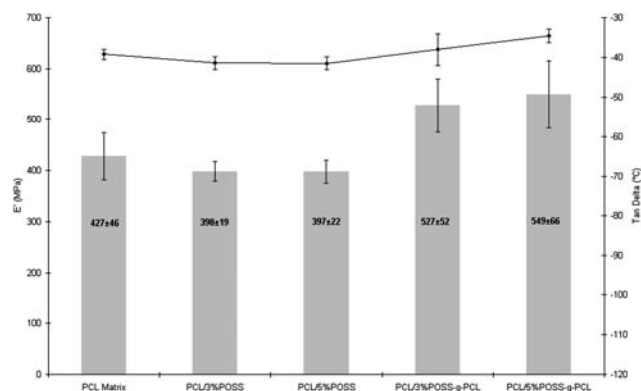


Fig. 6 The effect of filler content and PCL grafting on the storage modulus as determined at 20 °C.

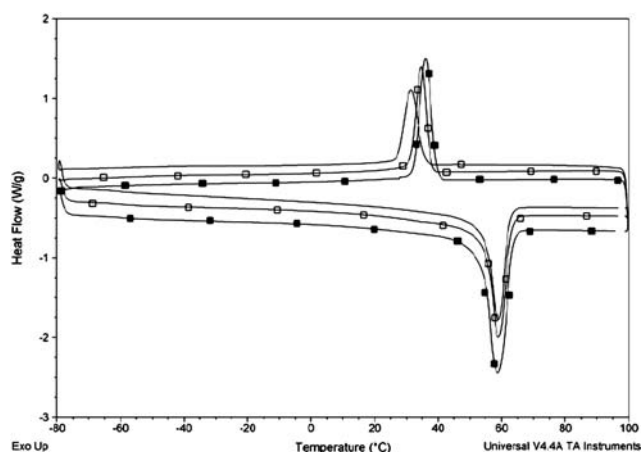


Fig. 7 DSC thermograms of PCL and related (nano)composites: (–) unfilled CAPA6500, (□) CAPA6500/5%aPOSS and (■) CAPA6500/5%aPOSS-g-PCL (recorded at 2nd cycle).

Further thermal characterizations were carried out by modulated temperature differential scanning calorimetry (MTDSC).⁴¹ The usefulness of quasi-isothermal crystallization experiments for the characterization of nanocomposite systems in general has already been demonstrated for EVA/carbon nanotube and polyamide/clay nanocomposites, where a reduced chain segment mobility of the matrix polymer could be revealed as a result of a pronounced matrix-filler interaction.^{42,43} For PCL nanocomposites, this methodology allowed evidencing of the profound changes exerted by well-dispersed nanofillers on the crystallization behaviour and crystalline morphology of the matrix polymer, as will be highlighted in a forthcoming publication.⁴⁴ As a matter of fact, both quasi-isothermal as well as non-isothermal studies lead to the same conclusions as to the beneficial effect of grafting PCL onto aPOSS nanoparticles: the improved properties result from the high density in nucleating sites and from the superior dispersion and compatibilization of PCL-grafted aPOSS within the commercial PCL matrix (CAPA 6500). In line with these results, the broadening of Tan Delta at the high-temperature end in DMTA experiments (Fig. 5) may be explained by the high crystallinity degree, restricting the relaxation of PCL chains. Accordingly, MTDSC experiments have indeed revealed the occurrence of a rigid amorphous fraction (RAF) in PCL nanocomposite systems.⁴⁴

Table 3 DSC analyses of unfilled CAPA6500, CAPA6500/aPOSS (3 and 5wt%) and CAPA6500/aPOSS-g-PCL (3 and 5 wt%) and a simple melt-blend CAPA6500/aPOSS(5wt%)/oligo-PCL. Heat/cool/heat from –80 to 100 °C with heating ramp of 10 °C min⁻¹

Samples	2nd cycle			
	T _g /°C	ΔH _c /J g ⁻¹	T _m /°C	ΔH _m /J g ⁻¹
CAPA6500	32	56	59	62
+3%aPOSS	34	69	61	74
+5%aPOSS	35	70	60	74
+3%aPOSS-g-PCL	35	83	58	84
+oligo-PCL/5%aPOSS	35	72	59	75
+5%aPOSS-g-PCL	36	88	59	92

Poly(lactide)/POSS nanocomposites

Taking advantage of the nucleating effect provided by polyester-grafted POSS, similar grafted aPOSS masterbatches were studied in the case of commercial PLA matrix (PLA4032D). In this respect, we purposely studied a P(L,L-LA)-based copolymer containing 10 wt% D,D-LA, exhibiting a low extent of crystallization in order to highlight the nucleating effect of polyester-grafted nanoparticles on the crystalline and thermo-mechanical properties of PLA. In order to achieve the best effect on crystalline properties, a loading of 5 wt% aPOSS-g-P(L,L-LA) in the commercial PLA matrix was maintained as previously reported in the case of aPOSS-filled PCL. Using the same “grafting from” approach (see Scheme 1), a poly(L,L-lactide)-grafted aPOSS (aPOSS-g-PLA) nanohybrid with a DP of 74 and an inorganic content of 14 mol% was synthesized by ring-opening polymerization of L,L-lactide at 80 °C for 7 h. PLA4032D-based materials were then prepared by melt-blending at 180 °C. For a sake of comparison, ⁱBu-POSS (iPOSS) (see Fig. 2) was studied as non-grafted (non reactive) POSS nanoparticles instead of using amino-POSS. During the melt-processing of PLA in the presence of amino-POSS, it was observed that the torque viscosity fell dramatically in comparison of neat PLA and PLA4032D/aPOSS-g-PLA materials. This indicated the partial degradation of PLA as explained by an aminolysis reaction between the primary amine function present on each POSS nanocage and the PLA matrix at high temperature. In contrast, ⁱBu-POSS-filled PLA were successfully prepared by melt-processing *via* twin-screw extrusion without observing any degradation of PLA.

Morphological investigations were first performed by high resolution TEM. In the case of PLA4032D/5%iPOSS, Fig. 8a clearly shows some partial association of nanoparticles, but still forming aggregates with average diameters in the 50 to 200 nm range. Interestingly, no aggregate could be detected in the case of PLA4032D/5%aPOSS-g-PLA sample (Fig. 8b).

The diffraction patterns of PLA4032D, PLA4032D/5%iPOSS and PLA4032D/5%aPOSS-g-PLA are reported in Fig. 9. As expected for highly amorphous polyester like the investigated PLA(90/10 L/D), a broad signal is observed on all WAXS spectra. WAXS diffractogram of PLA4032D/5%iPOSS is very similar to the WAXS spectrum recorded for neat PLA. In the low angle range, PLA4032D/5%iPOSS presents two signals corresponding to the high crystallinity related with the POSS association. This confirms the presence of POSS aggregates within the commercial PLA matrix. When the PLA4032D/5%aPOSS-g-PLA nanocomposite is observed, these diffraction peaks fully

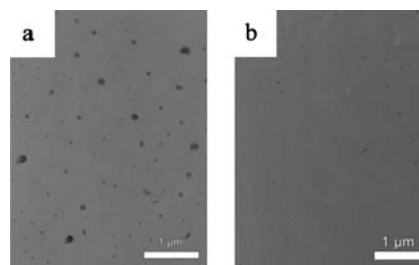


Fig. 8 HRTEM images of (a) PLA4032D/5%iPOSS and (b) PLA4032D/5%aPOSS-g-PLA-based (nano)composites.

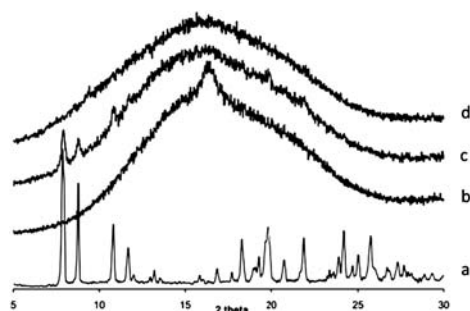


Fig. 9 WAXS spectra of (a) POSS nanoparticles, (b) unfilled PLA4032D, (c) PLA4032D/5%POSS and (d) PLA4032D/5%POSS-g-PLA.

vanish, attesting again for the complete POSS dissociation and the homogenous dispersion of individual inorganic nanoparticles throughout the polyester matrix. This confirms our HR-TEM observations.

Direct visual observation of the compression-molded PLA samples (either neat or filled with either aPOSS-g-PLA or PLA4032D/5%iPOSS) provides further confirmation of the extent of POSS dispersion within the commercial PLA matrix (Fig. 10). In contrast to the opaque and white PLA4032D/5%iPOSS (micro)composites, the grafted aPOSS-derived PLA nanocomposites appear clear and transparent. A fine dispersion of PLA-grafted aPOSS allowed preserving the inherent transparency of PLA matrix.

DTMA analyses were then carried out. Due to some uncontrolled crystallization phenomena of this specific (90/10 L/D) PLA matrix, it was highly difficult to get reproducible results by DMTA. All samples were therefore annealed at 110 °C for 90 min to get rid of these crystallization phenomena. Fig. 11 shows the isochronal evolution of the storage modulus (E') of so-annealed samples as a function of temperature. To compare the potential nucleating effect of POSS nanoparticles on the mechanical properties, DMTA analyses were carried out on both unfilled PLA4032D and (nano)compositions filled with either iPOSS or aPOSS-g-PLA (with 5 wt% inorganics). A rapid decrease of E' is noted around 70 °C, corresponding to the glass-rubber transition of the PLA matrix. Below T_g , no major modification for the storage modulus of different composites was noticed. Above 70 °C, the addition of POSS nanofillers leads to an increase of the storage modulus, which was higher when the aPOSS-g-PLA masterbatch was used. It is worth noting that at a temperature higher than 100 °C, a crystallization phenomenon

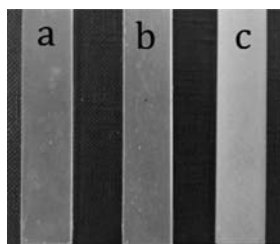


Fig. 10 Optical images of the compression-moulded PLA specimen samples: (a) unfilled PLA4032D, (b) PLA4032D/5%POSS-g-PLA and (c) PLA4032D/5%POSS (nano)compositions.

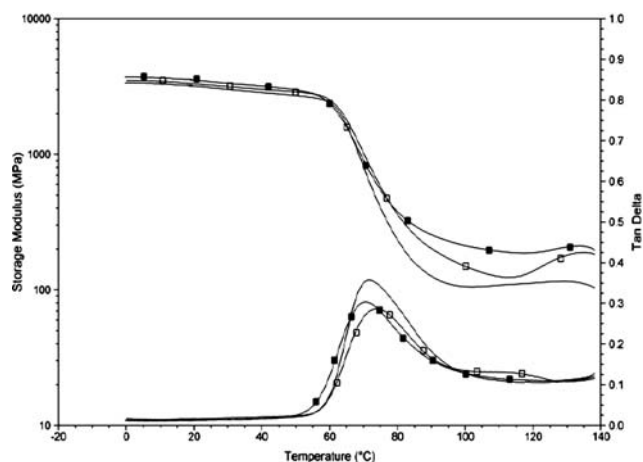


Fig. 11 Isochronal evolution of the storage modulus (E') vs. temperature of (–) unfilled PLA4032D, (■) PLA4032D/5%iPOSS and (□) PLA4032D/5%aPOSS-g-PLA (nano)compositions.

seems to occur and needs further investigations to be correctly interpreted (*vide infra*). As far as Tan Delta is concerned, its position is shifted towards a slightly lower temperature. This result is more likely to be due to a plasticization of the commercial PLA matrix by the presence of short PLA chains ($DP = 74$) grafted to the individually dispersed aPOSS nanocages (Table 4). The plasticization effect will also be highlighted by DSC as discussed in the following section.

Taking into account the very low rate of crystallization and degree of crystallinity of the studied PLA matrix, some nucleating effect provided by finely dispersed POSS nanoparticles is to be assumed. Indeed, DSC analyses confirm the low degree of crystallinity for the unfilled PLA matrix, even after annealing it at 110 °C for 90 min (Fig. 12). In presence of any POSS nanofillers, crystallization takes place within the commercial PLA matrix. In presence of 5 wt% iPOSS, a slight crystallization occurs, resulting in a melting enthalpy of 3 J g⁻¹. Interestingly, when aPOSS-g-PLA (again 5 wt% inorganics) is added, an important cold crystallization exotherm is observed. In other words, when individually dispersed, the PLA-grafted aPOSS nanoparticles allow substantially enhancing the rate of crystallization for the commercial PLA matrix. A melting enthalpy as high as 35 J g⁻¹ was accordingly recorded for the PLA matrix, although it contains 10 wt% of D,D-LA units randomly distributed along the P(L,L-LA) chains. It is worth noting that a double melting peak observed for PLA4032D/5%aPOSS-g-PLA is observed due to the possible presence of different crystal morphologies.⁴⁵

Clearly, masterbatch-based PLA nanocomposite materials take advantage of the covalent grafting between both partners, getting access to a good dispersion of aPOSS nanoparticles

Table 4 DMTA analyses: Tan Delta values

Samples	Tan Delta/°C
PLA4032D	73.6 ± 3.1
+5%iPOSS	75.9 ± 0.7
+5%aPOSS-g-PLA	69.4 ± 1.3

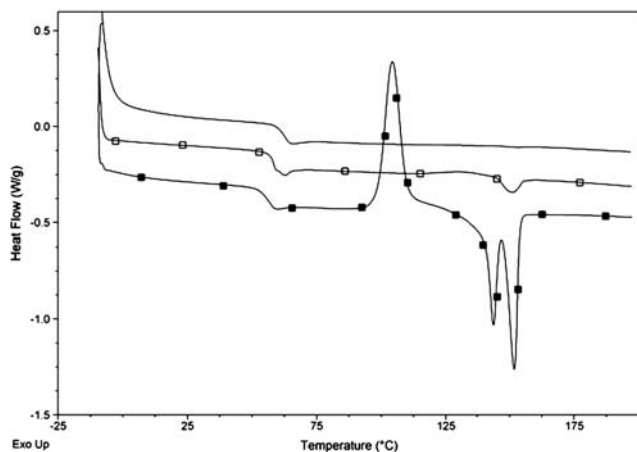


Fig. 12 DSC thermograms of annealed samples: (—) unfilled PLA4032D, (■) PLA4032D/5% iPOSS and (□) PLA4032D/5% aPOSS-g-PLA (nano)composites (recorded at 2nd cycle).

together with a significant nucleating effect. As far as T_g is concerned, the addition of non-grafted iPOSS affects slightly the glass-transition temperature compared to one of unfilled PLA matrix (Table 5 and Fig. 12). However, the use of the aPOSS-g-PLA masterbatch leads to a decrease of T_g , which can be explained by the plasticization of the commercial PLA matrix in the presence of the short aPOSS-grafted PLA chains ($M_n \approx 5,000 \text{ g mol}^{-1}$).⁴⁶

Conclusions

Polyester nanocomposites filled with individually dispersed POSS nanofillers were prepared *via* melt-blending using polyester-grafted amino-POSS nanohybrids as masterbatches in order to improve the crystallization degree of commercially available biodegradable polyester matrices, *i.e.*, PCL and PLA. aPOSS-g-PCL and aPOSS-g-PLA nanohybrids were produced by ring-opening polymerization (ROP) of the respective (di)lactone initiated by amino-functionalized POSS and using tin octoate ($\text{Sn}(\text{Oct})_2$) as catalyst.¹ After melt-blending with their corresponding commercial matrices, finely dispersed aPOSS nanoparticles were achieved, significantly enhancing the crystallinity and therefore the thermo-mechanical properties of these matrices. Indeed aPOSS nanoparticles proved by acting as efficient nucleating sites. The most relevant observation could be achieved on the crystalline properties of a selected PLA matrix containing 90 wt% L,L-LA and 10 wt% D,D-LA monomeric

Table 5 DSC analyses recorded on unfilled PLA4032D matrix, PLA4032D/iPOSS microcomposite and PLA4032D/aPOSS-g-PLA nanocomposite (5wt% inorganics). Heat/cool/heat from 0 to 220 °C with heating ramp of 10 °C min⁻¹

Samples	2nd cycle				
	$T_g/^\circ\text{C}$	$T_c/^\circ\text{C}$	$\Delta H_c/\text{J g}^{-1}$	$T_m/^\circ\text{C}$	$\Delta H_m/\text{J g}^{-1}$
Neat PLA	63	—	—	—	—
PLA/5% iPOSS	58	130	1	151	3
PLA/5% aPOSS-g-PLA	53	109	29	144/153	35

units randomly distributed along the chain, *i.e.*, a poorly crystallizable polylactide. Interestingly, incorporation of aPOSS-g-PLA nanoparticles within this selected PLA matrix (5 wt% aPOSS in the final nanocomposite) allowed for significantly improving the crystalline degree of the polyester matrix and therefore its mechanical performances.

Acknowledgements

The authors are grateful to the “Région Wallonne” and European Community (FEDER, FSE) in the frame of “Pôle d’Excellence Materia Nova” for their financial support. LPCM thanks the “Belgian Federal Government Office Policy of Science (SSTC)” for general support in the frame of the PAI-6/27. A.-L. Goffin thanks F.R.I.A. for her PhD thesis grant. J.-M. Raquez is “chargé de recherche” by the F.R.S.-FNRS. H. E. Miltner acknowledges the Research Foundation Flanders (FWO-Vlaanderen) for financial support.

Notes and references

- 1 A.-L. Goffin, E. Duquesne, S. Moins, M. Alexandre and Ph. Dubois, *Eur. Polym. J.*, 2007, **43**, 4103.
- 2 P. G. Harrison, *J. Organomet. Chem.*, 1997, **542**, 141.
- 3 www.hybridplastics.com.
- 4 Y. Zhang, S. Lee, M. Yoonessi, K. Liang and C. U. Pittman, *Polymer*, 2006, **47**, 2984.
- 5 M. Joshi and B. S. Butola, *Polymer*, 2004, **45**, 4953.
- 6 A. Fina, H. C. L. Abbenhuis, D. Tabuani, A. Frache and G. Camino, *Polym. Degrad. Stab.*, 2006, **91**, 1064.
- 7 B. X. Fu, L. Yang, R. H. Somani, S. X. Zong, B. S. Hsiao, S. Phillips, R. Blanski and P. Ruth, *J. Polym. Sci., Part B: Polym. Phys.*, 2001, **39**, 2727.
- 8 Y. Zhao and D. A. Schiraldi, *Polymer*, 2005, **46**, 11640.
- 9 S. H. Phillips, T. S. Haddad and S. J. Tomczak, *Curr. Opin. Solid State Mater. Sci.*, 2004, **8**, 21.
- 10 M. Z. Asuncion and R. M. Laine, *Macromolecules*, 2007, **40**, 555.
- 11 H. Rios-Dominguez, F. A. Ruiz-Trevino, R. Contreras-Reyes and A. Gonzales-Montiel, *J. Membr. Sci.*, 2006, **271**, 94.
- 12 S. Bourbigot, S. Duquesne and Ch. Jamal, *Macromol. Symp.*, 2006, **233**, 180.
- 13 A. Vannier, S. Duquesne, S. Bourbigot, A. Castrovinvi, G. Camino and R. Delobel, *Polym. Degrad. Stab.*, 2008, **93**, 818.
- 14 Lei Song, Qingliang He, Yuan Hu, Hao Chen and Lei Liu, *Polym. Degrad. Stab.*, 2008, **93**, 627.
- 15 A. Fina, D. Tabuani, A. Frache and G. Camino, *Polymer*, 2005, **46**, 7855.
- 16 L. Matejka, A. Strachota, J. Plestil, P. Whelan, M. Steinhart and M. Slouf, *Macromolecules*, 2004, **37**, 9449.
- 17 S. Y. Soong, R. E. Cohen and M. C. Boyce, *Polymer*, 2007, **48**, 1410.
- 18 M. E. Wright, B. J. Petteys, A. J. Guenther, S. Fallis, G. R. Yandek, S. J. Tomczak, T. K. Minton and A. Brunsvold, *Macromolecules*, 2006, **39**, 4710.
- 19 G. Pan, J. E. Mark and D. W. Schaefer, *J. Polym. Sci., Part B: Polym. Phys.*, 2003, **41**, 3314.
- 20 J. Mu, Y. Liu and S. Zheng, *Polymer*, 2007, **48**, 1176.
- 21 A. Strachota, I. Kroutilova, J. Kovarova and L. Matejka, *Macromolecules*, 2004, **37**, 9457.
- 22 A. Tsuchida, C. Bolln, F. G. Sernetz, H. Frey and R. Mülhaupt, *Macromolecules*, 1997, **30**, 2818.
- 23 J. Wang, Z. Ye and H. Joly, *Macromolecules*, 2007, **40**, 6150.
- 24 N. E. Markovic, M. Ginic-Markovic, S. Clarke, J. Matisons, M. Hussain and G. P. Simon, *Macromolecules*, 2007, **40**, 2694.
- 25 W. Xu, Ch. Chung and Y. Kwon, *Polymer*, 2007, **48**, 6286.
- 26 W. Kai, L. Hua, T. Dong, P. Pan, B. Zhu and Y. Inoue, *Macromol. Chem. Phys.*, 2008, **209**, 1191.
- 27 B. H. Yang, H. Y. Xu, C. Li and S. Y. Guang, *Chin. Chem. Lett.*, 2007, **18**, 960.
- 28 Y. Ni and S. Zhang, *J. Polym. Sci., Part B: Polym. Phys.*, 2007, **45**, 2201.

- 29 L. Ricco, S. Russo, O. Monticelli, A. Bordo and F. Bellucci, *Polymer*, 2005, **46**, 6810.
- 30 J. Xu and W. Shi, *Polymer*, 2006, **47**, 5161.
- 31 A. Fina, D. Tabuani, T. Peijs and G. Camino, *Polymer*, 2009, **50**, 218.
- 32 B. Lepoittevin, N. Pantoustier, M. Devalckenaere, M. Alexandre, D. Kubies, C. Calberg, R. Jerome and Ph. Dubois, *Macromolecules*, 2002, **35**, 8385.
- 33 G. Carrot, D. Rutot-Houze, A. Pottier, Ph. Degée, J. Hilborn and Ph. Dubois, *Macromolecules*, 2002, **35**, 8400.
- 34 J. Pyun, K. Matyjaszewski, J. Wu, G.-M. Kim, S. B. Chun and P. T. Mather, *Polymer*, 2003, **44**, 2739.
- 35 G. S. Constable, A. J. Lesser and E. B. Coughlin, *Macromolecules*, 2004, **37**, 1276.
- 36 Y. Ni and S. Zheng, *Macromolecules*, 2007, **40**, 7009.
- 37 Y. Liu, X. Yang, W. Zhang and S. Zheng, *Polymer*, 2006, **47**, 6814.
- 38 K. Zeng, L. Wang, S. Zheng and X. Qian, *Polymer*, 2009, **50**, 685.
- 39 Ph. Dubois, Ph. Degée, R. Jérôme and Ph. Teyssié, *Macromolecules*, 1992, **25**, 2614.
- 40 H. Hu and D. L. Dorset, *Macromolecules*, 1990, **23**, 4604.
- 41 H. E. Miltner, Ph.D. Thesis, Vrije Universiteit of Brussel, Belgium, 2008.
- 42 H. E. Miltner, S. Peterbroek, P. Viville, Ph. Dubois and B. Van Mele, *J. Polym. Sci., Part B: Polym. Phys.*, 2007, **45**, 1291.
- 43 H. E. Miltner, G. Van Assche, A. Pozsgay, B. Pukanszky and B. Van Mele, *Polymer*, 2006, **47**, 826.
- 44 H. E. Miltner, N. Watzeels, N.-A. Gotzen, G. Van Assche, B. Goderis, A.-L. Goffin, E. Duquesne, S. Benali, B. Ruelle, S. Peeterbroeck, Ph. Dubois, B. Van Mele., in preparation.
- 45 W. Hamley, V. Castelletto, R. V. Castillo, A. J. Muller, C. M. Martin, E. Pollet and Ph. Dubois, *Macromolecules*, 2005, **38**, 463.
- 46 M. Murariu, A. Da Silva Ferreira, M. Pluta, L. Bonnaud, M. Alexandre and Ph. Dubois, *Polym. Adv. Technol.*, 2008, **19**, 636.